Journal of Magnetic Resonance 298 (2019) 58–63

Contents lists available at ScienceDirect

Journal of Magnetic Resonance

journal homepage: www.elsevier.com/locate/jmr

Magnetic field gradient waveform correction of motion-sensitized SPRITE by pre-equalization

Alexander Adair, Frédéric G. Goora, Benedict Newling *

Department of Physics, University of New Brunswick, Fredericton, New Brunswick E3B5A3, Canada

ARTICLE INFO

Article history:
Received 22 August 2018
Revised 23 November 2018
Accepted 24 November 2018
Available online 27 November 2018

Keywords:
High-intensity pulsed field gradients
Eddy currents
Gradient waveform correction
Pre-equalization
Pure phase-encoding
Flow

ABSTRACT

Eddy currents caused by pulsed field gradients in magnetic resonance measurements of high-speed flow cause the magnetic field gradient amplitude waveform experienced by the sample to be different from the waveform demanded of the magnetic field gradient amplifiers. By measuring and using the system impulse response, pre-equalization magnetic field gradient waveform correction can be used to counteract the resulting errors in measured signal phase at the cost of minimal additional experimental time. The effectiveness of the pre-equalization method of magnetic field gradient waveform correction is tested with a motion-sensitized (pulsed field gradient) version of the SPRITE imaging pulse sequence which requires extreme gradient slew rates in excess of 1000 T/m/s in a 6.7-cm-bore set of gradient windings. Pre-equalized, motion-sensitized SPRITE is used to create velocity maps of high-speed (c. 4 m/s) water flow through a pipe constriction.

1. Introduction

The application of pure phase-encoding magnetic resonance imaging (MRI) to the study of flow systems has been previously demonstrated [1–4]. Purely phase-encoded MRI measurement techniques are able to image multiphase flow systems without image artifacts caused by magnetic susceptibility differences. In particular, motion-sensitized versions of the SPRITE (Single-Point Ramped Imaging with T_1-Enhancement) MRI pulse sequence have been shown to be well-suited to measuring fast, turbulent, multiphase flow systems [2].

Unlike traditional single-point imaging (SPI), the SPRITE pulse sequence incorporates ramping between sequential phase-encoding magnetic field gradient amplitudes, which greatly reduces the effects of eddy currents and allows for short repetition times on the order of milliseconds. However, significant eddy current effects are reintroduced when SPRITE is modified to include motion-sensitization through the use of pulsed field gradients (PFG). In particular for studying fast flow systems, motion-sensitized SPRITE includes the addition of bipolar gradient pulses onto the imaging gradient waveform at each phase-encoding interval [1]. Rapidly-switching, large-amplitude magnetic field gradients are inherent with this technique and, as a result, eddy current effects are significant [4–6].

Accurate calculations of velocity using this technique require accurate knowledge of the magnetic field gradient waveform experienced by the sample during the phase-encoding intervals. The true magnetic field gradient waveform experienced by the sample is not the same as the waveform demanded of the amplifiers (the input waveform) due to the eddy currents that are produced during the phase-encoding interval by the bipolar gradient pulse. Acquiring motion-sensitized SPRITE data without correcting for eddy current effects results in errors in both the measured k-space trajectory as well as the signal phase. The errors in signal phase cause errors in calculated velocity values, often to the point of nonsensical results.

Methods to compensate for eddy current effects (primarily through pre-emphasis or k-space regridding) have been previously established [7–15]. Eddy current compensation discussed in this paper uses the pre-equalization correction method [16], which involves a convolution process rather than the addition process typical of pre-emphasis. The pre-equalization method uses the impulse response of the system to calculate a specific input magnetic field gradient waveform that, as a result of the eddy currents present during a measurement, causes the sample to experience the desired waveform. In this paper, the existing method for correcting phase errors (pixel-by-pixel subtraction of the phase in an image of stationary fluid [1]) is compared with the pre-equalization correction method. The pre-equalization method greatly reduces phase errors caused by eddy currents and allows for the creation of accurate velocity maps using motion-

* Corresponding author.
E-mail addresses: adair.alex@unb.ca (A. Adair), f.goora@unb.ca (F.G. Goora), bnewling@unb.ca (B. Newling).

https://doi.org/10.1016/j.jmr.2018.11.007
1090-7807/

sensitized SPRITE in significantly less measurement time than the stationary-data method.

2. Theory

SPRITE is a pure phase-encoding MRI measurement technique which has been used to perform a wide variety of measurements [17]. In order to measure velocity, motion-sensitization is added to SPRITE by superimposing a bipolar PFG (pulsed field gradient) at each phase-encoding interval (see Fig. 1), which provides motion-sensitized information for each measured k-space data point. Given the bipolar pulse timings and amplitudes shown in Fig. 1, and assuming a constant mean velocity v in the flowing sample, phase can be expressed as

$$\begin{aligned}\phi &= \gamma \int_0^{t_p} \vec{G}(t)\cdot\vec{r}(t)\,dt \\ &= \gamma t_p\left[G(r_0+\tfrac{1}{2}vt_p)+\tfrac{1}{4}g v t_p\right]\end{aligned} \tag{1}$$

where G is the amplitude of the imaging gradient, r_0 is position, and t_p is the phase-encoding time interval (typically 0.5–1 ms).

The phase calculation shown in Eq. (1) assumes that the bipolar gradient pulse during the phase-encoding interval is as shown in Fig. 1. However, the amplitude switching of the bipolar gradient pulse, in the presence of nearby conductive structures, results in the creation of eddy currents. The induced eddy currents generate magnetic fields which oppose the changing magnetic field caused by the bipolar gradient pulse, which results in a finite gradient rise time. Therefore, it is impossible to obtain the instantaneous gradient amplitude switching shown in Fig. 1. Eddy currents in a motion-sensitized SPRITE measurement cause the two lobes of the bipolar PFG pulses to have different sizes than intended and to be of different size when compared with one another [4–6].

The incorrect size of the two lobes of the bipolar gradient pulse causes errors in calculated velocity values. An existing method for correcting such errors is the use of a stationary data set [1]. In this approach, all measurements are performed once with the sample flowing and again with the sample stationary. The measured phase is a combination of the phase due to motion and the error in phase due to the incorrect bipolar gradient pulses ($\phi_{\text{measured}} = \phi_{\text{motion}} + \phi_{\text{error}}$). The phase from a stationary (no motion) data set directly reports the phase error and a subtraction corrects the measured phase, which is then used to create velocity maps for the flowing sample. Besides the significant downside of requiring twice the experimental time, the stationary-data method does not correct for errors in the path of the measured k-space trajectory that are caused by the imbalance in the sizes of the two lobes of the bipolar pulse. One effect of this imbalance, for example, is that the first acquired point in a motion-sensitized Spiral SPRITE measurement is no longer the k-space origin—the benefits of a centric-scan measurement (e.g., simplified contrast information) [18] have been lost.

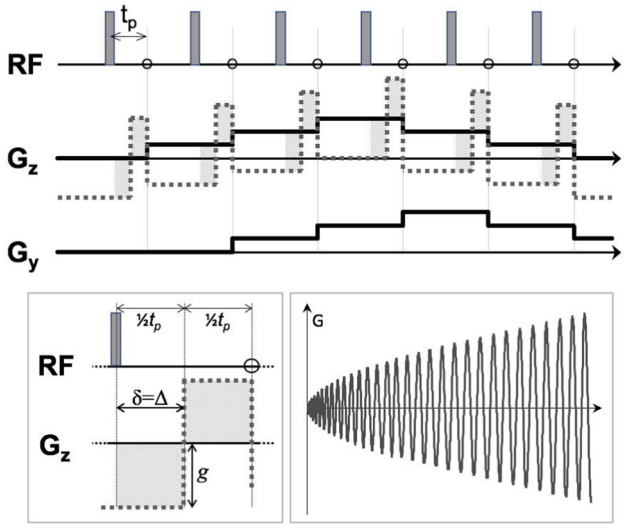

Fig. 1. [Top] Schematic of the first few points in a 2D Spiral SPRITE pulse sequence. Motion-sensitization is applied in the z-direction by superimposing bipolar gradient pulses (marked with diagonal hatching) onto the imaging gradient G_z. The (non-pre-equalized) magnetic field gradient waveform demanded of the amplifiers is shown as the dotted line on G_z. [Bottom-left] A phase-encoding interval of the pulse sequence, showing bipolar pulse timings $\delta = \Delta = \frac{1}{2}t_p = 295$ μs and amplitude g. [Bottom-right] The complete G_z waveform (shown without motion-sensitizing pulses) is approximately six seconds in duration.

The stationary-data method corrects velocity data post-measurement but makes no attempt to better control the gradient waveform experienced by the sample during the measurement. Simple adjustments to the amplitude or width of the gradient pulses can be attempted to reduce the mismatch between the size of the two lobes [4–6]. This method can greatly reduce any mismatch, but may still result in small errors due to the reliance on manual correction [4]. Other methods for changing the magnetic field gradient waveform to compensate for eddy current effects are also common. The pre-emphasis method fits the decay of the magnetic field gradient following a gradient pulse to a superposition of multiple exponential functions. Choosing the proper time constants and amplitudes of those exponential functions greatly reduces the eddy current effects of the magnetic field gradient delivered by the gradient coils [7–9]. More recent pre-emphasis techniques that employ the system impulse response have also been developed [10,11]. The pre-equalization correction method also controls the behavior of the magnetic field gradient experienced by the sample by using measured information about the eddy current response, but does so through a convolution method rather than the addition method common to pre-emphasis. Pre-equalization ensures that the bipolar gradient pulses experienced by the sample are balanced in size and match the expected behavior that is used for velocity calculations. The impulse response of the system is measured separately prior to velocity measurements and used to calculate the input (the *pre-equalized* gradient waveform) necessary to achieve the desired output (the gradient waveform experienced by the sample) [16]. The pre-equalized gradient waveform x_p is given by

$$x_p(t) = \mathcal{F}^{-1}\left\{\frac{\mathcal{F}[y_d(t)]}{\mathcal{F}[h(t)]}\right\} \tag{2}$$

where y_d is the desired gradient waveform to be experienced by the sample, h is the system impulse response, $\mathcal{F}^{-1}$ denotes the inverse Fourier transform, and $\mathcal{F}$ is the Fourier transform.

3. Experimental

Measurements were performed using a 4.7 T vertical bore superconducting magnet (Cryomagnetics, TN, USA) and a Redstone HF NMR spectrometer console (Tecmag, TX, USA). Magnetic field gradients were generated with a homemade magnetic field gradient set (with an inner bore diameter of 5.08 cm), driven by Techron 7700 Series power supply amplifiers (AE Techron, IN, USA). The gradient set is capable of generating magnetic field gradients in three orthogonal spatial directions (x, y, and z). At maximum current, the gradient amplitudes available are $G_x = 0.66$ T/m, $G_y = 0.54$ T/m, and $G_z = 0.72$ T/m. Radio frequency (RF) excitations were accomplished using a Doty DSI-874 RF ^{1}H probe (Doty Scientific, SC, USA), driven by an AMT M3205A RF amplifier (American Microwave Technology, CA, USA). A glass pipe, with an inner diameter of 17.3 mm, was placed vertically inside the magnet bore and

positioned such that a constriction in the pipe (with a minimum inner diameter of 5.5 mm ± 0.1 mm) was within the sensitive region of the RF probe (see Fig. 2).

The flowing liquid was distilled water doped with $CuSO_4$. Bulk relaxation time constant measurements using a standard inversion-recovery technique gave a T_1 of 20 ms. The water was pumped from a reservoir (where it was maintained at 12 °C ± 0.5 °C) vertically down through the glass pipe using a BPDH10-L centrifugal pump (Berkley, WI, USA). The flow rate (measured using a mechanical flow meter to be 6.0 Lpm ± 0.4 Lpm), was kept below the threshold flow rate that would have caused hydrodynamic cavitation at the constriction. The RF probe was sufficiently far within the magnet that the flowing sample reached equilibrium magnetization before reaching the imaging region.

Images were acquired using the Spiral SPRITE pulse sequence, which is a 2D, centric-scan version of the pure phase-encoding SPRITE MRI measurement technique [19]. A phase-encoding time interval $t_p = 590$ μs was used to create 2D ^{1}H density images of the sample. The time necessary to acquire one scan of k-space was approximately six seconds. Sixteen scans were acquired for each image and averaged together to improve SNR, resulting in a total measurement time of approximately 1.5 min per image. Images were acquired in the zy-plane orientation (the z-axis is along the length axis of the pipe). The imaging field of view was 5.7 cm in the z-direction and 1.6 cm in the y-direction. The nominal spatial resolution for the images was 0.9 mm in the z-direction and 0.25 mm in the y-direction. Using the maximum flow speed of 4 m/s ± 0.5 m/s (which is the estimated flow speed at the constriction throat, calculated from the volumetric flow rate), the liquid travels 1.2 mm ± 0.2 mm during the motion-encoding interval $\frac{1}{2}t_p = 295$ μs. This corresponds to a distance traveled in the z-direction of approximately 1.3 pixels, which results in smearing/misregistration artifacts in the images. There is no misregistration in regions where the flow speed is low enough that the distance traveled during the motion-encoding interval is less than the size of a pixel (this corresponds to flow speeds below 3 m/s).

Spatially-resolved velocity data were acquired with motion-sensitization applied solely in the z-direction by adding bipolar pulses to the z-imaging gradient. If desired, the experiment can be repeated with bipolar pulses applied in any other direction in order to measure that component of velocity. Velocity information was gathered by performing a series of measurements with seventeen different bipolar pulse gradient amplitudes g (see Fig. 1). The data were zero-filled to thirty-two points and an inverse Fourier transformation along the dimension defined by g generated a center-of-mass propagator for each pixel in the 2D image [20–22]. Fig. 3 shows an example center-of-mass propagator taken from the center point of the velocity map in Fig. 6B. The peak value in each center-of-mass propagator was assigned as the modal displacement for that pixel, but no other interpretation of the center-of-mass propagator shape was attempted [20–22]. The modal velocity was determined by dividing the modal displacement by the motion-encoding interval $\frac{1}{2}t_p$. The nominal velocity resolution in the velocity maps is 0.32 m/s. Switching the gradient amplitude from $-g$ to g during the bipolar pulses occurred over 200 μs. For the maximum value of g used for this experiment (0.2 T/m), the gradient slew rate was 2000 T/m/s, which is a dB/dt of 60 T/s at 3 cm (half the field of view in the z-direction). For comparison, a typical maximum slew rate for a medical MRI system is 200 T/m/s which is a dB/dt of 70 T/s at the bore radius of 35 cm [23].

Two separate experiments (with the same flow conditions) were performed to compare the different correction methods. For the stationary-data method, two sets of data were acquired for all seventeen (different g amplitudes) motion-sensitized Spiral SPRITE measurements. One set of data was acquired with the liquid flowing. For the other set of data, the pump was shut off and the liquid was not flowing. The signal phase measured from the stationary data set is the error in phase due to the presence of eddy currents during the measurement. Therefore, the phase information from the stationary data set was subtracted from the phase information from the flowing data set during data processing to remove the error. The corrected phase was then used to create velocity maps.

The second method used the pre-equalization technique to correct for the phase error due to eddy currents. The magnetic field gradient monitor (MFGM) technique was used to measure the response of the system to a gradient amplitude step input [24,25]. Other gradient waveform measurement processes have also been used for pre-emphasis correction methods [12,14]. Differentiating the system response to the gradient step resulted in the system impulse response, $h(t)$ [16]. This information was used according to Eq. (2) to generate a magnetic field gradient waveform

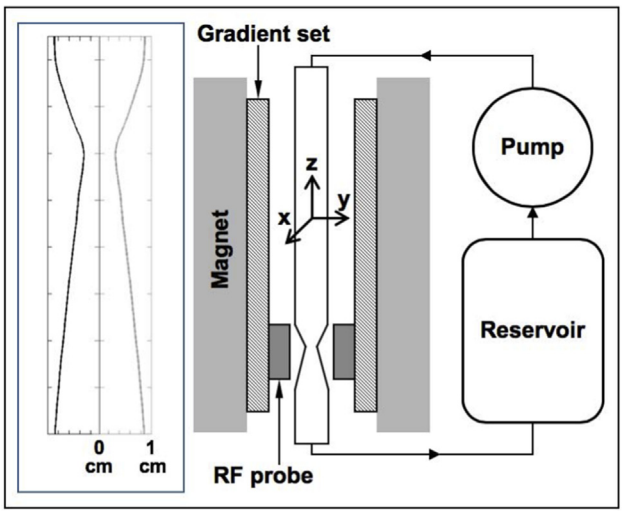

Fig. 2. A schematic of the apparatus showing the glass pipe oriented vertically (in the z-direction) within the magnet. The contour of the constriction is shown at the left.

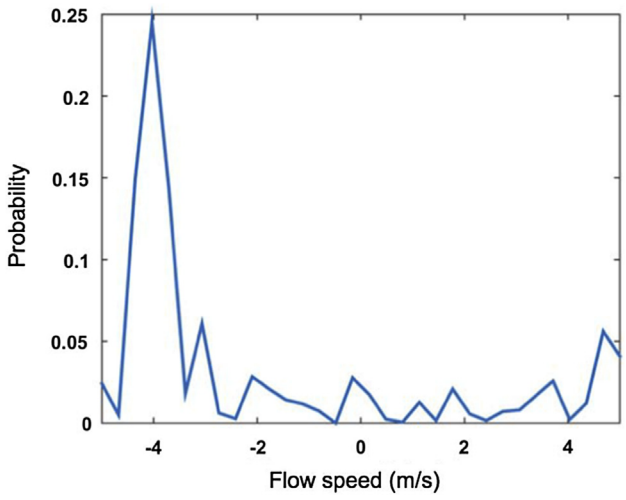

Fig. 3. An example center-of-mass propagator taken from the center point of the velocity map of Fig. 6B. The horizontal axis, in m/s, is the displacement divided by $\Delta = \frac{1}{2}t_p$. The vertical axis is probability. The only physical interpretation of the center-of-mass propagator that was used was the choice of maximum probability to represent the modal velocity in a pixel [20–22].

(the pre-equalized waveform, $x_p(t)$), which, as a result of convolution with the impulse response, causes the sample to experience the desired gradient waveform, $y_d(t)$. The desired gradient waveform is selected to conform to the limits of gradient amplifier slew rate and bandwidth.

Including data processing and MFGM measurements, a system impulse response can be obtained in a few hours. However, it is only necessary to obtain the system impulse response once for a given apparatus configuration [16]. Some variation in the impulse-response of the system with temperature might be expected, but has proven too small to be noticeable in velocity measurements made so far. This is in contrast to observable changes caused by changing the RF probe, for example. Pre-equalized magnetic field gradient waveforms were generated for all seventeen (different g amplitudes) motion-sensitized Spiral SPRITE measurements. These pre-equalized waveforms were used to measure the flowing sample and the resulting data were used to create velocity maps of the flow system.

4. Results and discussion

Fig. 4 shows the behavior of the magnetic field gradient waveform with and without pre-equalization. If the desired waveform is used as input, the sample experiences an undesired, distorted output (characterized by slower-than-desired switching due to eddy currents). However, by using the pre-equalized waveform as input, the sample can be made to experience a waveform that closely matches the desired waveform. Although Fig. 4 shows only one amplitude of the gradient switching, pre-equalization has been shown to apply over a range of gradient values [16]. Some nonlinear behavior is expected (due, in part, to gradient amplifier performance and thermal variation in the system), but agreement between results and expectations show that any nonlinear behavior is small enough that linearity can be assumed [16]. The behavior of the pre-equalized waveform is as expected—since eddy currents reduce the gradient amplitude switching rate, the pre-equalized waveform starts switching earlier and at a higher rate in order to achieve the desired output.

A feature of the eddy-current compromised magnetic field gradient that is experienced by the sample is that the two lobes of the bipolar pulse are of unequal sizes. A consequence of this imbalance is that the net magnetic field gradient amplitude during each phase-encoding interval is shifted from its intended value, which shifts the measured k-space trajectory away from its expected path. For the case of Spiral SPRITE (a centric-scan measurement), the first k-space point collected should be the k-space origin. However, due to the unequal lobe sizes, the net gradient amplitude for the first acquired point is non-zero and the k-space origin is not acquired until later in the waveform (i.e., it is no longer a centric-scan measurement, which removes the benefits of simplified contrast and improved signal-to-noise ratio that come with the centric approach [18]). The stationary-data method does not correct the lobe size imbalance prior to measurements; therefore, it cannot fix the issues that result in a non-centric-scan measurement. On the other hand, the pre-equalization method is able to correct the lobe size imbalance, which results in a measurement having the correct k-space trajectory. Representations of the measured 2D k-space data for four different, uncorrected motion-sensitized SPRITE measurements are shown in Fig. 5. The motion-sensitizing bipolar gradient pulses are applied to the G_z imaging gradient. Fig. 5A shows the k-space data that arises from a measurement with $g = 0$ (i.e., no motion-sensitization)—the k-space peak is at the center of the measured spiral trajectory, as expected. When g is increased (Fig. 5B), the imbalance in the bipolar gradient lobe sizes causes the measured trajectory to shift along the k_z axis (i.e., the k-space peak is shifted away from the center of the measured spiral trajectory). When g is further increased (Fig. 5C and D), the shift also increases. For extremely large g, the shift can be large enough that the k-space origin data point is not acquired at all.

Velocity maps of the flowing sample are shown in Fig. 6(A–C). Fig. 6A is the velocity map that is created by using motion-sensitized Spiral SPRITE without any form of correction. The results clearly show incorrect results for water flow through the pipe constriction. Fig. 6B is the velocity map that is created by using the pre-equalization method to correct the magnetic field gradient

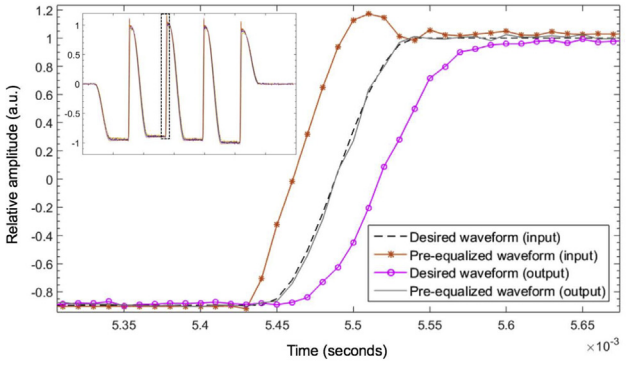

Fig. 4. Input and output gradient waveforms for part of a motion-sensitized Spiral SPRITE measurement showing the gradient switching that occurs during a phase-encoding interval. The desired waveform is shown as the dashed line. Using the desired waveform as the input to the gradient amplifier produces the line marked with circles as the output gradient experienced by the sample. Using a pre-equalized waveform as input (marked with asterisks) produces the solid line as output, which closely matches the desired waveform. Output waveforms were measured using MFGM [24]. The x-axis is in units of seconds and data points occur every 10 μs. The y-axis is normalized to the maximum amplitude of the desired waveform (which is 88 mT/m in this case). The desired waveform has a slew rate of approximately 1600 T/m/s. The inset shows the complete waveform that was used. The main plot focuses on the behavior of the second phase-encoding interval, as shown.

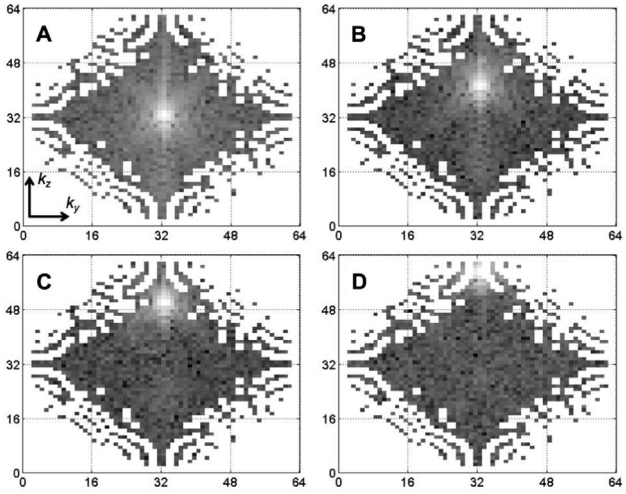

Fig. 5. Natural logarithm (arbitrary units) of acquired 2D k-space data for uncorrected, motion-sensitized Spiral SPRITE with different bipolar pulse amplitudes g. Motion-sensitization is applied in the z-direction. The amplitude g is zero for (A) (i.e., no motion-sensitization) and increases incrementally through (B), (C), and (D) (amplitudes of 0.07 T/m, 0.13 T/m, and 0.20 T/m, respectively). The k-space span is 17.6 m^{-1} in the z-direction and 62.7 m^{-1} in the y-direction for 64 × 64 2D k-space. Size difference between the lobes of the bipolar gradient pulses cause the measured k-space trajectory to shift away [(B), (C), and (D)] from its intended path (A). For extremely large g [i.e., greater than that of (D)], the measured k-space trajectory can shift sufficiently far that it does not acquire the k-space origin data point.

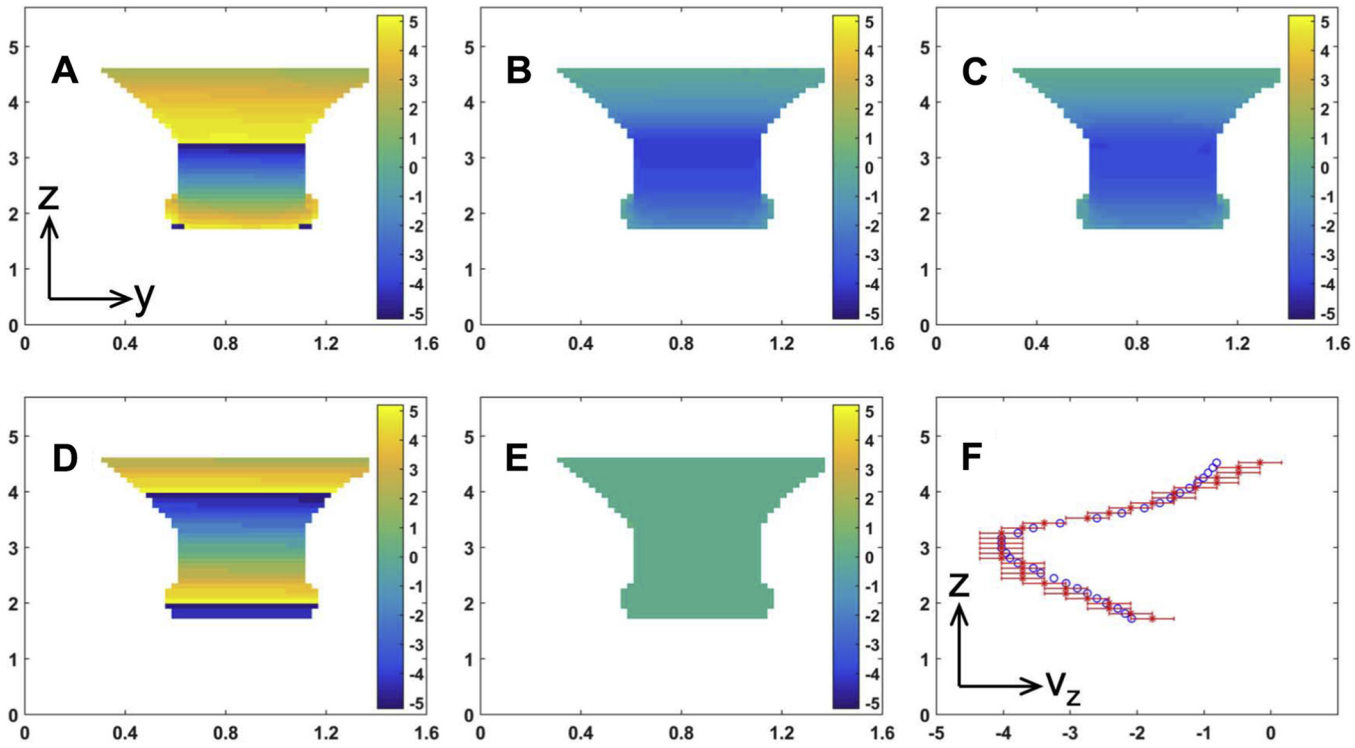

Fig. 6. Maps of the z-component of velocity for water flowing vertically down through a pipe constriction. (A–E) The spatial (zy) axes have units of centimeters and the velocity values have units of meters per second. The velocity maps are of (A) Flowing sample with no correction, (B) Flowing sample with pre-equalization correction, (C) Flowing sample with stationary-data method correction, (D) Non-flowing sample with no correction, and (E) Non-flowing sample with pre-equalization correction. The uncorrected velocity maps show nonsensical data. The corrected velocity maps show expected behavior with flow speeds reaching a peak value of 4 m/s at the constriction throat for the flowing sample and uniform 0 m/s for the non-flowing sample. A noise threshold mask was used with the velocity maps to remove noise outside the pipe. (F) Shows agreement between the centerline velocity along the pipe axis for the pre-equalization correction method (* symbols) and centerline velocity based on the pipe diameter and volume flow rate (o symbols). Velocity resolution in the pre-equalization correction map is shown as error bars on the centerline data. The z-axis has units of centimeters and the y-axis has units of m/s (color images available).

waveform prior to data acquisition. The velocity map shows reasonable results; the flow speed is higher in regions of the pipe with smaller diameter and the maximum flow speed agrees with the expected flow speed at the constriction throat of 4 m/s ± 0.5 m/s (calculated from the volumetric flow rate and constriction throat diameter). Fig. 6C is the velocity map that is created by using the stationary-data method to correct for phase errors during data processing. Again, the velocity map shows reasonable results, with behavior similar to the velocity map corrected using the pre-equalization method. Despite strong similarity, the velocity maps shown in Fig. 6B and C are not identical. A possible cause of this is that although the stationary-data method is able to isolate phase that results from fluid motion, the exact shape of the bipolar waveform experienced by the sample is unknown, compromising accurate velocity quantification. Therefore, calculations of modal velocity that are performed using the expected timing and amplitude parameters yield incorrect results.

Fig. 6D and E are velocity maps created of a stationary sample (therefore, with a known flow speed of 0 m/s throughout the sample). Fig. 6D is the velocity map with no correction method, which shows nonsensical results, as expected. Fig. 6E is the velocity map of the stationary sample that is created by using the pre-equalization correction method. It shows the expected results of a uniform flow speed of 0 m/s across the sample. This confirms (within the current velocity resolution of 0.32 m/s) that our assumptions about linearity over a range of g values are valid. Fig. 6F shows the agreement between the centerline velocities along the axis of the pipe calculated from the pre-equalization-corrected velocity map (Fig. 6B) and from the known pipe diameter and volume flow rate.

Total experiment time is also important to consider for the two correction methods. Acquiring all seventeen (different g amplitudes) motion-sensitized Spiral SPRITE measurements resulted in a total measurement time of approximately 30 min. The pre-equalization method requires no additional measurement time once the system impulse response has been measured for a given combination of magnet, gradient set and probe. The stationary-data method, on the other hand, requires acquiring twice the number of measurements. The doubling of measurement time is even more of a disadvantage if 3D velocity maps are attempted or if a large number of averages are needed to improve the signal-to-noise ratio (for example, with a gas sample). Another advantage of the pre-equalization method is that there are circumstances in which the stationary-data method is wholly impractical (i.e., some multiphase samples cannot be prepared in a stationary state such as in sprays [26] or cavitation).

5. Conclusion

Two-spatial-dimension images of water flowing through a pipe constriction were created using the Spiral SPRITE MRI pulse sequence. Bipolar magnetic field gradient pulses were superimposed onto the imaging gradient waveform to provide motion-encoding and velocity maps of the flow were created.

The bipolar gradient pulses used to motion-sensitize the Spiral SPRITE pulse sequence introduce large-amplitude, rapid-switching magnetic field gradients into the measurements. The resulting eddy currents that are created by these bipolar pulses cause the magnetic field gradient waveform experienced by the sample to be different than the waveform that the user demands from the

gradient amplifiers. Due to the altered behavior of the magnetic field gradient waveform experienced by the sample, the measured signal phase cannot directly be used to calculate velocity information.

Two methods of correcting for phase errors due to the presence of eddy currents were presented. The stationary-data method from the literature [1] is able to remove the phase error during data processing, allowing the creation of velocity maps; however, the process requires measurements when the sample is stationary as well as when it is flowing, which doubles measurement time and may be impossible for some samples (such as in sprays or cavitation). The pre-equalization method uses prior knowledge of the system impulse response to ensure that the magnetic field gradient waveform experienced by the sample is as desired, which improves accuracy. This method is presented here for the first time in application to improve velocity measurements, even in the presence of extreme gradient slew rates. A benefit of the pre-equalization method is that it does not require the significant additional experimental time that is needed for that stationary-data method.

Acknowledgments

The authors would like to thank the Natural Sciences and Engineering Research Council of Canada for financial support through the NSERC Postgraduate Scholarship (A.A.) and Discovery Grant (B.N.) programs [RGPIN-2017-04564].

References

[1] B. Newling, C.C. Poirier, Y. Zhi, J.A. Rioux, A.J. Coristine, D. Roach, B.J. Balcom, Velocity imaging of highly turbulent gas flow, Phys. Rev. Lett. 93 (15) (2004) 154503, https://doi.org/10.1103/PhysRevLett.93.154503.
[2] M. Sankey, Z. Yang, L. Gladden, M.L. Johns, D. Lister, B. Newling, SPRITE MRI of bubbly flow in a horizontal pipe, J. Magn. Reson. 199 (2009) 126–135, https://doi.org/10.1016/j.jmr.2009.01.034.
[3] I.V. Mastikhin, A. Arbabi, B. Newling, A. Hamza, A. Adair, Magnetic resonance imaging of velocity fields, the void fraction and gas dynamics in a cavitating liquid, Exp. Fluids 52 (2012) 95–104, https://doi.org/10.1007/s00348-011-1209-9.
[4] A. Adair, I.V. Mastikhin, B. Newling, Motion-sensitized SPRITE measurements of hydrodynamic cavitation in fast pipe flow, Magn. Reson. Imaging 49 (2018) 71–77, https://doi.org/10.1016/j.mri.2017.12.025.
[5] P. Galvosas, F. Stallmach, G. Seiffert, J. Kärger, U. Kaess, G. Majer, Generation and application of ultra-high-intensity magnetic field gradient pulses for NMR spectroscopy, J. Magn. Reson. 151 (2001) 260–268, https://doi.org/10.1006/jmre.2001.2381.
[6] F. Stallmach, P. Galvosas, Spin echo NMR diffusion studies, Annu. Rep. NMR Spectrosc. 61 (2007) 51–131, https://doi.org/10.1016/S0066-4103(07)61102-89.
[7] M.A. Morich, D.A. Lampman, W.R. Dannels, F.T.D. Goldie, Exact temporal eddy current compensation in magnetic resonance imaging systems, IEEE Trans. Med. Imaging 7 (1988) 247–254, https://doi.org/10.1109/42.77893.
[8] P. Jehenson, M. Westphal, N. Schuff, Analytical method for the compensation of eddy-current effects induced by pulsed magnetic field gradients in NMR systems, J. Magn. Reson. 90 (1990) 264–278, https://doi.org/10.1016/0022-2364(90)90133-T.
[9] J.J. Van Vaals, A.H. Bergman, Optimization of eddy-current compensation, J. Magn. Reson. 90 (1990) 52–70, https://doi.org/10.1016/0022-2364(90)90365-G.
[10] N.O. Addy, H.H. Wu, D.G. Nishimura, Simple method for MR gradient system characterization and k-space trajectory estimation, Magn. Reson. Med. 68 (2012) 120–129, https://doi.org/10.1002/mrm.23217.
[11] S.J. Vannesjo, M. Haeberlin, L. Kasper, M. Pavan, B.J. Wilm, C. Barmet, K.P. Pruessmann, Gradient system characterization by impulse response measurements with a dynamic field camera, Magn. Reson. Med. 69 (2013) 583–593, https://doi.org/10.1002/mrm.24263.
[12] G.F. Mason, T. Harshbarger, H.P. Hetherington, Y. Zhang, G.M. Pohost, D.B. Twieg, A method to measure arbitrary k-space trajectories for rapid MR imaging, Magn. Reson. Med. 38 (1997) 492–496, https://doi.org/10.1002/mrm.1910380318.
[13] P. Börnert, H. Schomberg, B. Aldefeld, J. Groen, Improvements in spiral MR imaging, Magn. Reson. Mater. Phys., Biol. Med. 9 (1999) 29–41, https://doi.org/10.1016/S1352-8661(99)00038-1.
[14] C. Barmet, N. De Zanche, K.P. Pruessmann, Spatiotemporal magnetic field monitoring for MR, Magn. Reson. Med. 60 (2008) 187–197, https://doi.org/10.1002/mrm.21603.
[15] S.J. Vannesjo, Y. Duerst, L. Vionnet, B.E. Dietrich, M. Pavan, S. Gross, C. Barmet, K.P. Pruessmann, Gradient and shim pre-emphasis by inversion of a linear time-invariant system model, Magn. Reson. Med. 78 (2017) 1607–1622, https://doi.org/10.1002/mrm.26531.
[16] F.G. Goora, B.G. Colpitts, B.J. Balcom, Arbitrary magnetic field gradient waveform correction using an impulse response based pre-equalization technique, J. Magn. Reson. 238 (2014) 70–76, https://doi.org/10.1016/j.jmr.2013.11.003.
[17] B.J. Balcom, R.P. MacGregor, S.D. Beyea, D.P. Green, R.L. Armstrong, T.W. Bremner, Single-point ramped imaging with T_1 enhancement (SPRITE), J. Magn. Reson. Ser. A 123 (1996) 131–134.
[18] I.V. Mastikhin, B.J. Balcom, P.J. Prado, C.B. Kennedy, SPRITE MRI with prepared magnetization and centric k-space sampling, J. Magn. Reson. 136 (1999) 159–168.
[19] M. Halse, D.J. Goodyear, B. MacMillan, P. Szomolanyi, D. Matheson, B.J. Balcom, Centric scan SPRITE magnetic resonance imaging, J. Magn. Reson. 165 (2003) 219–229, https://doi.org/10.1016/j.jmr.2003.08.004.
[20] P.P. Mitra, B.I. Halperin, Effects of finite gradient-pulse widths in pulsed-field-gradient diffusion measurements, J. Magn. Reson. Ser. A 113 (1995) 94–101, https://doi.org/10.1006/jmra.1995.1060.
[21] W.S. Price, NMR Studies of Translational Motion, Cambridge University Press, Cambridge, 2009.
[22] J.M. Pope, S. Yao, Quantitative NMR imaging of flow, Concepts Magn. Reson. 5 (1993) 281–302, https://doi.org/10.1002/cmr.1820050402.
[23] Philips Ltd., View details of Philips Ingenia 1.5T. http://www.philips.ca/healthcare/product/HC781341/ingenia-15t-mr-system (accessed March 30, 2017).
[24] H. Han, R.P. MacGregor, B.J. Balcom, Pure phase encode magnetic field gradient monitor, J. Magn. Reson. 201 (2009) 212–217, https://doi.org/10.1016/j.jmr.2009.09.011.
[25] F.G. Goora, B.J. Balcom, Accuracy of the magnetic field gradient waveform monitor technique and consequent accuracy of pre-equalized gradient waveforms, Concepts Magn. Reson. B 46B (2016) 67–80, https://doi.org/10.1002/cmr.b.21323.
[26] I.V. Mastikhin, K.M. Bade, S. Ahmadi, A rapid magnetization preparation for MRI measurements of sprays, J. Magn. Reson. 283 (2017) 52–60, https://doi.org/10.1016/j.jmr.2017.08.011.